Theory of Unimolecular Dissociation of Small Metastable Molecules and Ions As Exemplified by H_3^+

ELI POLLAK*

Chemical Physics Department, Weizmann Institute of Science, Rehovot 76100, Israel

CHRISTOPH SCHLIER

Fakultät für Physik, Universität Freiburg, D-7800 Freiburg, Federal Republic of Germany

Received November 4, 1988 (Revised Manuscript Received March 20, 1989)

I. Introduction

The word "metastable" has traditionally been used to denote states that decay with a much slower rate than what is "normally" expected. For example, in atomic spectroscopy, states that emit photons of visible light at a rate much slower than the usual 10^8 s^{-1} are called metastables. Metastability in atomic spectroscopy is generally due to selection rules.

Mass spectra of molecular ions consist of fragmentation patterns of a mother ion, generally produced by electron impact or by laser photoionization. Mother ions that undergo slow decay (i.e., in microseconds instead of picoseconds) are called metastable ions,[1,2] and they are observable as fractional masses in the mass spectrometer. Metastable unimolecular decay of excited neutral molecules is also expected, but measurement is more difficult than in ion fragmentation. However, in principle there is no difference between neutrals and ions in the dynamics described below.

The specific example that initiated our work on metastable unimolecular decay[3-13] is H_3^+. Marvelous experiments on the photodissociation of this ion have been done by A. Carrington and his group, and some of these are described in this issue.[14] In these experiments, photodissociation comes from (single) photon excitation of H_3^+ ions followed by unimolecular decomposition of the excited H_3^+. The photodissociation spectrum between 870 and 1090 cm^{-1} consists of 27 000 lines. The measured line widths indicate that both states involved in the transitions have lifetimes of 1 ns to 1 μs. In contrast to these results, the translational energy of the fragments measured by Carrington and Kennedy indicates that in many cases even the lower state of the transition lies up to 2000 cm^{-1} (250 meV) above the dissociation energy ($H_3^+ \rightarrow H^+ + H_2$). A naive RRKM prediction for 250 meV above dissociation gives 3 ps as an order of magnitude estimate for the lifetime.

The photodissociation spectrum has an average line density of 120 per cm^{-1} and no simple assignable structure. However, clusters of lines are observed. As a result, when the spectrum is coarse grained into a pseudo-low-resolution spectrum, four peaks are found to be centered at 876, 928, 978, and 1034 cm^{-1}. As a final surprise, in the spectrum of HD_2^+, for which H^+ and D^+ products can be observed separately, it is found that a single transition produces either a state decaying into $H^+ + D_2$ or one decaying into $D^+ + HD$, but not both channels simultaneously.

Many questions arise: What is the reason for the strong metastability of 3–6 orders of magnitude? What are the dynamics of the decay? How can there be so many metastable states? Why does metastable HD_2^+ not decay simultaneously into D^+ and H^+? What makes the spectrum cluster about certain frequencies?

It is quite clear from theory[15,16] and experiment[14,17] that the metastability of H_3^+ is not a result of excitation to a weakly coupled vibronic manifold of levels. H_3^+ also differs considerably from weakly coupled van der Waals molecules where, because of weak vibrational coupling, there exist dynamic barriers to energy redistribution that cause metastability.[18] H_3^+ is a strongly bound molecule. Classical trajectory computations[13] show that the bulk of unimolecular decay in H_3^+ is fast and is not hindered by dynamic barriers in phase space. Rotational predissociation, i.e., tunneling through a rotational barrier, that arises from the orbiting motion of the fragments was proposed in 1968 by Rosenstock[19] and later by Klots[20] as the explanation of observed

Christoph G. Schlier was born in 1930 in Jena (now GDR). He studied physics at Tübingen and Bonn, where he earned his Ph.D. in 1956. After an interlude in high-energy physics at CERN and Bonn, he turned to molecular beam scattering experiments. This work was continued when he became Professor of Physics at the University of Freiburg in 1963, and he shifted to ion beam scattering in the mid 1970s. Work on H^+–H_2 scattering turned his interest to theoretical methods of treating long-lived collision intermediates.

Eli Pollak was born in Haifa, Israel, in 1950. He studied Talmud in Yeshivat Merkaz Harav and Physics and Chemistry at the Hebrew University, Jerusalem, where he received his Ph.D. in 1977. At present he is an Associate Professor at the Weizmann Institute, where he has been since 1979. His main professional interests are the theory of molecular collisions, transition-state theory, and nonlinear dynamics in condensed phases.

(1) Hipple, J. A.; Fox, R. E.; Condon, E. U. *Phys. Rev.* **1946**, *69*, 347.
(2) Brenton, A. G.; Morgan, R. P.; Benyon, J. H. *Annu. Rev. Phys. Chem.* **1979**, *30*, 51; cf. especially p 66 ff.
(3) Schlier, Ch.; Vix, U. *Chem. Phys.* **1985**, *95*, 401. Schlier, Ch. *Mol. Phys.* **1987**, *62*, 1009.
(4) Pollak, E. *J. Chem. Phys.* **1987**, *86*, 1645 L.
(5) Berblinger, M.; Pollak, E.; Schlier, Ch. *J. Chem. Phys.* **1988**, *88*, 5643.
(6) Gomez Llorente, J. M.; Pollak, E. *Chem. Phys. Lett.* **1987**, *138*, 125.
(7) Berblinger, M.; Schlier, Ch. *Mol. Phys.* **1988**, *63*, 779.
(8) Gomez Llorente, J. M.; Pollak, E. *Chem. Phys.* **1988**, *120*, 37.
(9) Gomez Llorente, J. M.; Pollak, E. *J. Chem. Phys.* **1988**, *89*, 1195 L.
(10) Gomez Llorente, J. M.; Pollak, E. *J. Chem. Phys.*, in press.
(11) Berblinger, M.; Gomez Llorente, J. M.; Pollak, E.; Schlier, Ch. *Chem. Phys. Lett.* **1988**, *146*, 353.
(12) Berblinger, M.; Schlier, Ch.; Pollak, E. *J. Phys. Chem.* **1989**, *93*, 2319.
(13) Berblinger, M. Ph.D. Thesis, to be published.
(14) Carrington, A.; McNab, I. R. *Acc. Chem. Res.*, preceding paper in this issue and references therein.
(15) Köppel, H.; Domcke, W.; Cederbaum, L. S. *Adv. Chem. Phys.* **1984**, *57*, 59.
(16) Schaad, L. J.; Hicks, W. V. *J. Chem. Phys.* **1974**, *61*, 1934.
(17) Carrington, A.; Kennedy, R. A. *J. Chem. Phys.* **1984**, *81*, 91.
(18) Davis, M. J.; Gray, S. K. *J. Chem. Phys.* **1986**, *84*, 5389.
(19) Rosenstock, H. M. In *Advances in Mass Spectroscopy*; Kendrick, E., Ed.; Institute of Petroleum: London, 1968; p 542.

0001-4842/89/0122-0223$01.50/0

metastability in several small ions. The major problem with this explanation was that, for polyatomic systems, orbital angular momentum is not conserved. One is not really sure what, in this case, an orbital angular momentum barrier really means.

Much effort[3-13,21-23] has been put into answering the questions posed by the experimental photodissociation spectrum of H_3^+. The resulting theory is quite general and applies to the metastable decay of many neutral and ionic molecules (the recently published metastable decay of Ar_3^+ clusters is an obvious example[24]). In this Account, we will demonstrate the principles on one specific system, metastable H_3^+. Section II explains qualitatively the rotational dynamics leading to metastability. Here, the important new concept is the *total* angular momentum barrier. In section III we show how total angular momentum barriers lead to quantitative estimates and provide answers to the questions posed by the experimental probe of the unimolecular decay of H_3^+. Since we are dealing with a polyatomic molecule at high energies for which exact quantal solutions are still prohibitive, it was necessary to develop reliable but approximate theoretical tools, some of which are also briefly described in this section. Section IV describes our classical mechanical interpretation of the coarse-grained spectrum. Finally, section V summarizes those questions that still need to be resolved both theoretically and experimentally.

II. Total Angular Momentum Barriers

As noted in the Introduction, orbital angular momentum is not conserved for a system with three or more atoms. However, the total angular momentum (denoted by J) is a constant of the motion. To rotate a molecule, energy must be expended. This means that the effective configuration space available to the molecule will be critically dependent on the angular momentum. To see this more clearly, one must estimate quantitatively the minimal energy that is tied up in the rotational motion. For a fixed molecular configuration (denoted by $\mathbf{x}$) one can look for those values of the momenta that *minimize the kinetic energy of the system subject to the constraint of conservation of total angular momentum.* We denote the resulting minimum energy by $U_J^{\min}(\mathbf{x})$. If we initiate a classical trajectory somewhere else on the potential energy surface, with the same J but with an energy lower than $U_J^{\min}(\mathbf{x})$, this trajectory will never be able to visit the configuration $\mathbf{x}$. Chesnavich[25] and Rynefors and Nordholm[26] used this principle to map out "forbidden regions" of configuration space as a function of energy and J.

For any breakup channel of the molecule, we can identify a "reaction coordinate" (R) as the distance between the center of mass of the two fragments and denote all other coordinates by $\mathbf{x}'$. If we now further minimize the Hamiltonian over all values of $\mathbf{x}'$ but at fixed R, we will obtain an effective potential $U_J^{\min}(R)$ which depends on J and R. Examples of such effective potentials are shown in Figure 1. For $J \neq 0$, the effective potentials have barriers at large values of R and wells at smaller values. We will see that a plot of the J barriers is an immediate source of very important information that goes a long way toward explaining many of the features of the Carrington and Kennedy experiments.

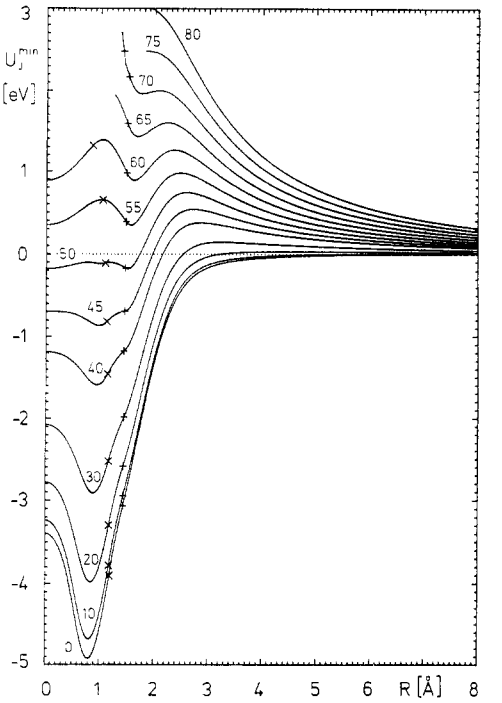

Figure 1. Minimal effective potential energy curves $U_J^{\min}(R)$ calculated from the DIM potential energy surface of H_3^+. The parameter is total angular momentum. The main difference between the DIM potential and the true one is only a 7% deeper well. The crosses indicate the change in geometrical configuration at the minimum. From $R = 0$ to $R = x$, the configuration is perpendicular ($\gamma = \pi/2$), from $R = +$ to $R = \infty$ it is collinear ($\gamma = \pi$), and in between there is a smooth change.

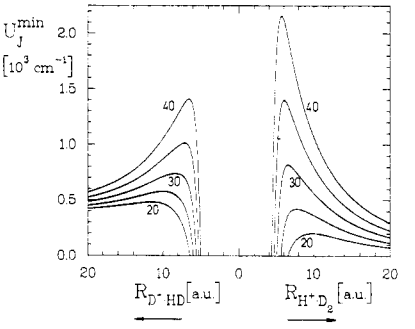

Figure 2. Minimal total angular momentum barriers for the two decay channels of HD_2^+:D^+ + HD to the left, and H^+ + D_2 to the right. The parameter is J. Note that the energy is referred to the zero-point level of D_2, and that the zero point energy shift of HD has been included.

Consider first the observation of metastability. Suppose that, for a given J, the barrier of $U_J^{\min}(R)$ is at $R^\ddagger$ with energy $U_J^\ddagger$. Any classical trajectory initiated at $R < R^\ddagger$ and $E < U_J^\ddagger$ will never be able to cross the barrier. Such a trajectory will never lead to the fragments whose "reaction coordinate" is R. For a symmetric system such as H_3^+ where all three fragmentation channels are identical by symmetry, it becomes clear that for $E < U_J^\ddagger$ and $R < R^\ddagger$ such a trajectory will never be able to dissociate, although its energy could

(20) Klots, C. E. *Chem. Phys. Lett.* **1971**, *10*, 422.
(21) Child, M. S. *J. Phys. Chem.* **1986**, *90*, 3595.
(22) Pfeiffer, R.; Child, M. S. *Mol. Phys.* **1987**, *60*, 1367.
(23) Chambers, A. V.; Child, M. S.; Pfeiffer, R. *J. Chem. Soc., Faraday Trans. 2* **1988**, *84*, 1305.
(24) Maerk, T. D. *J. Chem. Phys.* **1988**, *89*, 295.
(25) Chesnavich, W. J. *J. Chem. Phys.* **1982**, *77*, 2988.
(26) Rynefors, K.; Nordholm, S. *Chem. Phys.* **1985**, *95*, 345.

be much higher than the asymptotic dissociation energy into $H^+ + H_2$. The same is true in asymmetric systems (cf. Figure 2) when, at a given J, the energy E is below the J barriers of all fragmentation channels. It is this result that is crucial to understanding the phenomenon of metastable molecules and ions.[4,5] Quantum mechanically, the trapping lifetime will be finite because of tunneling through the J barriers. Since these barriers are usually quite broad, and the masses of the fragments are large, tunneling lifetimes can become very long even at energies slightly below the J barrier.

The J barriers plotted in Figure 1 also provide immediate and fascinating information on the existence of J-dependent geometrical isomers of the same molecule or ion. For example, inspection of Figure 1 for the H_3^+ system shows that the geometry of the J-dependent minima changes from an equilateral triangle at low J to a collinear configuration at high J. Spinning the molecule very quickly tends to straighten it out. For larger molecules, this effect can give a very rich series of different geometrical isomers of the same molecule that differ only by their total angular momentum.[27]

Isotopic selectivity such as found in D_2H^+, or, more generally, channel-specific chemistry, can be understood in terms of total J barriers.[11,12] As an example we will consider in some detail isotope separation in a triatomic system. For a triatomic ABC there are three arrangement channels (A + BC, AB + C, AC + B). One can associate with each channel a set of three internal coordinates (R_i, r_i, γ_i), where R_i is defined as above, r_i is the diatom internuclear distance, and γ_i is the angle between R_i and r_i. The minimum effective potential at fixed J (cf. Figure 2) is given by the relation

$$U_J^{\min}(R_i) = \min_{r_i,\gamma_i} \left\{ V(R_i,r_i,\gamma_i) + \frac{J^2}{2(M_iR_i^2 + m_ir_i^2)} \right\} \quad (1)$$

where M_i is the reduced mass for the R_i motion (i.e., for A + BC, $M_i = m_Am_{BC}/m_{ABC}$) and m_i is the reduced mass of the diatom. Since the barriers are located, for most J, at R values that are much larger than r, one can approximate the moment of inertia appearing in eq 1 by MR^2. Consider then the system HD_2^+, which can dissociate into HD + D^+ or $D_2 + H^+$. $M(D^+)$ is larger than $M(H^+)$ so that for the same J the barrier leading to the D^+ channel will be lower than that leading to the H^+ channel. However, the zero-point energy of D_2 is lower than the zero-point energy of DH; therefore, at $J = 0$, the threshold for formation of H^+ is lower than for formation of D^+. It follows that for low J's the metastable HD_2^+ will decay predominantly into the H^+ channel. However, as J increases, the J barrier in the H^+ channel will rise faster than the D^+ barrier (cf. Figure 2), such that for $J > 30$ the D^+ barrier is lower than the H^+ barrier, and metastable HD_2^+ will decay predominantly into the D^+ channel. This selectivity is a quantum effect that depends on the zero-point energy of the products.

The selectivity with respect to J is critically dependent on the fact that we are studying metastables whose decay is by tunneling and thereby exponentially dependent on the barrier height. Usually, over 99% of the metastables will tunnel through the lowest barrier. If the energy is above the J barriers, then competition between the various channels will take place, with branching ratios that are of the order of 1.

J barriers can also be used to estimate the J dependence of product energy distributions in metastable decay.[8,10,12] The barriers are usually far in the exit channel where the motion of the two fragments is, to a good approximation, separable. The lifetime of the metastable is determined primarily by the probability of tunneling through the barrier. Since this probability depends exponentially on the energy available for motion in the R direction, decay occurs primarily with a maximal amount of energy in translation. At a given E,J an excellent rule of thumb is that the products' translational energy will be maximal, with very little internal rotational or vibrational excitation. This fact can be used (in conjunction with the lifetime) to invert the products' translational energy into a determination of the total angular momentum of the decaying metastable state.

In summary, a plot of the J barriers enables a very quick and qualitative determination of four important aspects of metastable chemistry: the energy and J range leading to metastables, the possible J-dependent geometrical isomers, the selectivity with respect to decay into the various product channels, and the products' translational energy distribution.

III. Unimolecular Decay of Metastable H_3^+

a. The Density of Metastable States. One of the big surprises of the Carrington and Kennedy experiments was the very large number of observed lines in the photodissociation spectrum. It is necessary to establish that the density of metastable states (i.e., states with total angular momentum J whose energy is greater than the dissociation threshold to $H^+ + H_2$ but less than the total J barrier height) is large enough to be compatible with the multitude of experimental lines.

It is well-known that the microcanonical versions of statistical theories, especially those of unimolecular decay (RRKM theory, quasiequilibrium theory), need, as their input, state densities of the activated molecule and state counts at the transition state. The difficulty in evaluating densities stems from the fact that at best there are only approximate quantum mechanical methods to calculate all quantum states of any strongly bound polyatomic molecule.[23]

The standard method is to count quantum states approximated by a separable harmonic oscillator, rigid rotor model plus some corrections for anharmonicity and sometimes for tunneling.[28] While this is quite reliable at low energies (which in large polyatomic molecules may well be above the first dissociation energy), we do not expect it to be a good approximation for a strongly coupled triatomic at energies near or above dissociation. Here the correspondence principle, which says that the average state density of a quantum system is given by its classical limit (sometimes called "semiclassical after Rice–Marcus"), comes to the rescue. It suffices to evaluate the classical phase space volume $V_J(E)$ at fixed E and J. The classical phase space is spanned by the coordinates and momenta of the classical mechanical Hamiltonian. This classical estimate becomes quite accurate as soon as E surpasses suffi-

(27) Jellinek, J.; Li, D. H. *Phys. Rev. Lett.* **1989**, *62*, 241.

(28) Robinson, P. J.; Holbrook, K. A. *Unimolecular Reactions*; Wiley: New York, 1972; p 131.

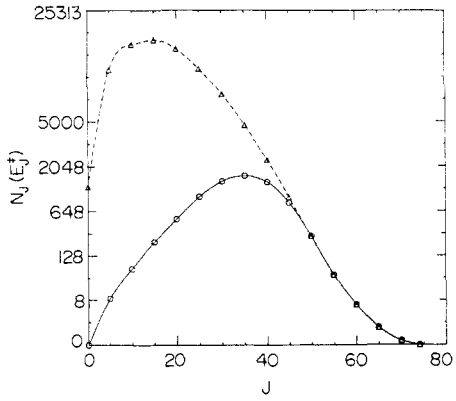

Figure 3. Classical number of states ($N_J(E_J^{\ddagger})$) below the minimal centrifugal barriers of H_3^+ at given total angular momentum J. Full line: only metastable states, i.e., states with $E > 0$, which decay by tunneling. Dashed line: all states. Note the nonlinear abscissa scale.

ciently the zero-point energy of the system.

Our method of evaluation[5,13] is a multidimensional Monte Carlo integration of the phase-space volume $V_J(E)$, constrained by fixing E and J. The number of quantum states corresponding to this volume is

$$N_J(E) = V_J(E)/h^{d/2} \qquad (2)$$

where d is the dimension of the phase space ($d = 12$ for H_3^+). The results for $N_J(E)$ can be easily interpolated (since $N_J(E)$ is a smooth and monotonic function of E) and also differentiated to give the density of states $\rho_J(E)$. Monte Carlo has been used previously to compute phase-space volumes at fixed total J.[29] We use straight Monte Carlo sampling, but work in the body fixed frame. This allows us to integrate four variables analytically before sampling and two numerically after sampling. (This leaves us with a six-dimensional Monte Carlo integration which can be speeded up by careful programming and the use of Halton's method[13] to produce quasirandom vectors.) As a result, the accuracy of integration is easily fixed to 2%, which allows us to treat them as virtually error free when computing lifetimes or any other phase-space average.

In Figure 3 we show a plot of the J dependence of the number of states. Here $N_J(E_J^{\ddagger})$ is the number of classical states with total angular momentum J whose energy is lower than the total J barrier height $E_J^{\ddagger}$. The triangles (and dashed interpolation line) show *all* states, including those whose energy is lower than the dissociation threshold at $E = 0$. The number of metastable states (open circles and solid line) is found by subtracting all states with energy $E < 0$ from $N_J(E_J^{\ddagger})$. We find up to 1200 metastable states per J, altogether there are at least 5000 metastable states within the experimental lifetime window. This is enough to account for the observed line density.

b. Tunneling Rates. Classical mechanically, all states trapped behind the total J barriers are truly bound states, even if their energy is greater than the threshold for dissociation into $H^+ + H_2$. Quantum mechanically, these states are metastable; the finite lifetime is determined by tunneling through the total J barrier. It is not yet possible to obtain numerically exact quantal decay rates; the system is just too big, so

(29) See, e.g.: Farantos, S. C.; Murrell, J. N.; Hajduk, J. C. *Chem. Phys.* **1982**, *68*, 109.

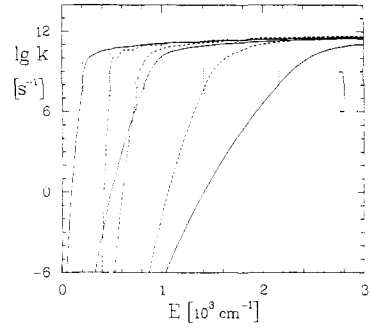

Figure 4. Unimolecular decay rates of HD_2^+ vs total energy for total angular momenta $J = 20$, 30, and 40 (from left to right) as computed by sudden TST including zero-point energies. Full lines: $H^+ + D_2$. Dashed lines: $D^+ + HD$. Dotted vertical lines are at the minimal centrifugal barriers while the bracket at right shows the experimental observation window (cf. ref 14).

one must use approximate methods.

In our studies, two complementary approaches were used. One method, which we call the classical tunneling trajectory (CTT) method,[8] is based on extension[30] of a method used for classical trajectory simulations of reactions on multiple electronic surfaces (known as the trajectory surface hopping technique).[31] The basic idea is that tunneling occurs when the classically allowed trajectory "hits the barrier" to dissociation. A long trajectory of duration time T will hit the barrier at different times t_i. At the ith hit there is a probability P_i for tunneling. If this trajectory samples "all" regions of classically allowed phase space (if it is ergodic), then the tunneling rate is estimated by the very simple formula

$$k_{uni}(E) = \lim_{T\to\infty} \frac{1}{T}\sum_i P_i \qquad (3)$$

The only real difficulty is the estimate of the tunneling probabilities P_i. A reasonable semiclassical estimate is based on a sudden approximation. One assumes that the phase-space variables perpendicular to the tunneling degree of freedom remain frozen during the tunneling process. This provides an effective one-degree-of-freedom Hamiltonian along the tunneling path for which the semiclassical tunneling probability is evaluated, using a one-dimensional quadrature.

The strong point of the CTT method is that the classical dynamics within the classically allowed region are treated exactly. The main drawback of the method is that one cannot account for the products' zero-point energy in a consistent manner. In classical mechanics, products can be formed at energies below the zero-point vibrational energy of the diatom. For heavy systems this might not be too important; for a system such as H_3^+, this is crucial. It was therefore necessary to complement the CTT method with a more approximate sudden transition state theory[11,12] (TST), which can be formulated with and without zero point energy corrections. When ignoring zero-point energies, the sudden TST estimate for the rate is found to be in very good agreement with the CTT estimate. This means that the sudden TST estimates, with zero point energy corrections, should be a reasonable approximation for the exact quantal rates. (A different method that gives

(30) Waite, B. A.; Miller, W. H. *J. Chem. Phys.* **1980**, *73*, 3713; **1981**, *74*, 3910.

(31) Tully, J. C.; Preston, R. K. *J. Chem. Phys.* **1971**, *55*, 562.

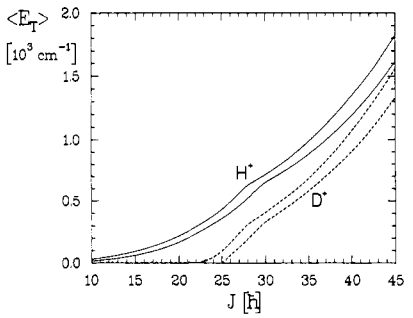

Figure 5. Average kinetic energy of the products (full lines, $H^+ + D_2$; dashed lines, $D^+ + HD$) of the unimolecular decay of HD_2^+ vs total angular momentum as computed by sudden TST (cf. Figure 4). The curves show these energies at a fixed decay rate of 10^6 s^{-1} (upper curve) and 10^9 s^{-1} (lower curve of each pair).

similar results may be found in ref 32.) An important advantage of the sudden TST method is that the computer time needed to implement it is substantially less than that for the CTT method.

Figure 4 shows the rates for the two channels of the HD_2^+ system obtained from the sudden TST, when the zero-point energy of the fragment diatomic is taken into account. At the lowest energies, the rate of formation of D^+ is identically 0, since the energy is below the threshold for formation of ground vibrational state HD. Here the zero of energy is at the threshold for formation of $D_2(n=0)$, and this is of course lower than the energy for formation of $HD(n=0)$. Only when J is about 30 do we find that the $k_J(E)$ curves for both channels cross, indicating that there is only a small region of J values where both channels are formed simultaneously. For other J's, the curves do not cross and either H^+ is formed (low J's) or D^+ is formed (high J's), as discussed in section II.

c. Product Translational Energies and Isotope Effects. In the experiments, there is no direct observation of the total angular momentum. However, there is an additional observable, the products' translational energy E_T. In principle, every single line has a translational energy distribution associated with it. The sudden TST and the CTT method can be used to predict this distribution; details may be found in ref 8, 11, and 12. We find that the distribution is usually sharply peaked about the average $\langle E_T \rangle$, which is itself close to the total energy. This is a consequence of the exponential dependence of the tunneling probability on the translational energy E_T. The larger E_T, the closer is the barrier top and the more probable is the tunneling process.

In Figure 5, instead of showing $\langle E_T \rangle$ as a function of E and J, we show it as a function of J and the unimolecular dissociation rate k for two typical values of k. The two values are the observational bounds in the experiments. Note that a given $\langle E_T \rangle$ is correlated with only a small range of J values as a result of the narrow experimental lifetime window. This implies that the measured $\langle E_T \rangle$ may be inverted into a total J. The reverse is also true. For example, since $J < 27$ leads predominantly to the H^+ product and since for this J the $\langle E_T \rangle$ of D^+ is 286 cm^{-1}, we can predict that, whenever D^+ is observed, its $\langle E_T \rangle$ will be greater than 286 cm^{-1}. Conversely, since H^+ is not formed for $J \geq 31$, and for this J, $\langle E_T \rangle = 680$ cm^{-1}, we predict that H^+ will not be detected with higher $\langle E_T \rangle$.

These predictions can be tested experimentally, and this should be accomplished in the near future. The predictions have a very practical aspect to them. For example, suitable setting of the electrostatic analyzer in the photodissociation experiment could lead to a very good isotopic separation of H^+ and D^+. The mechanism underlying this separation is very simple: the only important element is the difference in the threshold energies for formation of the two products. Such threshold differences will also exist in other systems, not necessarily only as a result of isotopic shifts. As already noted in section II, different J's may lead to different isomers with different decay routes. The separation of more complicated systems remains a challenge for the future.

IV. The Coarse-Grained Spectrum

The difficulty in interpretation or assignment of the measured 27 000 lines is the typical situation also in the very high overtone spectroscopy of neutral molecules. A quantum mechanical solution to the problem would be to diagonalize the exact Hamiltonian of the system. This is not possible mainly because the necessary computer power is not yet available. It is also not easy to digest a table with thousands of numbers. Therefore it is necessary to condense the data somehow. This is done by some form of coarse graining, usually by convolution with a smooth line shape. In H_3^+, this convolution leads to four prominent, equally spaced peaks. In other systems, this led to the identification of typical correlation times.[33] The theory for these phenomena has not yet been thoroughly clarified, although progress is being made.[33-36] Our general philosophy has been[6,10] that, with such a high density of states, classical mechanics should suffice for at least a qualitative understanding of coarse-grained spectra. In the following, we briefly describe our studies on the H_3^+ system. Again, the methodology is applicable to highly excited molecules in general and has only recently found an application in the analysis of the stimulated emission pumping spectrum of Na_3.[36]

The experimental setup in H_3^+ is such that, for a given laser frequency ω, one can, in principle, observe the transitions to all possible final states E_f whose lifetime is within the experimental window, from all possible initial states E_i such that the energy difference is $\hbar\omega = E_f - E_i$. Selection rules demand additionally that i and f must be states such that $\Delta J = J_f - J_i = 0$ or ± 1. From the correspondence principle one knows that, on the average, this spectrum is just the Fourier transform of the classical microcanonical dipole moment correlation function $\langle \vec{\mu}(0) \cdot \vec{\mu}(t) \rangle$, where $\vec{\mu}(t)$ is the dipole moment vector travelling along a classical trajectory of given total energy E and total angular momentum J. The brackets $\langle\ \rangle$ indicate that the correlation function has to be averaged over the whole accessible phase space. However, as already noted in the previous section, at the energies involved in the experiment, classical

(32) Chambers, A. V.; Child, M. S. *Mol. Phys.* **1988**, *65*, 1337.

(33) Pique, J. P.; Engel, Y. M.; Levine, R. D.; Chen, Y.; Field, R. W.; Kinsey, J. L. *J. Chem. Phys.* **1988**, *88*, 5972 L.

(34) Wintgen, D. *Phys. Rev. Lett.* **1987**, *58*, 1589. Wintgen, D.; Friedrich, H. *Phys. Rev. A* **1987**, *36*, 131.

(35) Gomez Llorente, J. M.; Zakrzewski, J.; Taylor, H. S.; Kulander, K. C. *J. Chem. Phys.* **1988**, *89*, 5959.

(36) Gomez Llorente, J. M.; Taylor, H. S.; Pollak, E. *Phys. Rev. Lett.*, in press.

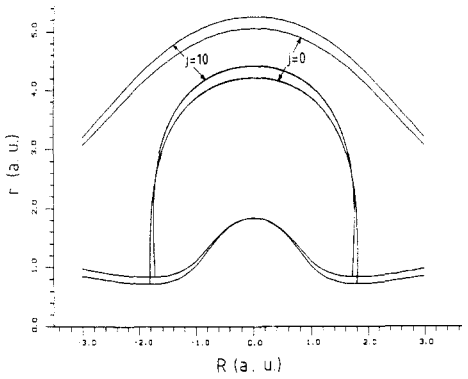

Figure 6. Rotating "horseshoe" orbits. Two orbits with equal action are shown for $j = 0$ and 10 with their respective equipotential energy contours at $E = 0$ and 2982 cm^{-1}, respectively.

motion behind the J barriers is chaotic. A single trajectory, integrated over long times, practically visits all of phase space, implying that it should suffice to integrate one trajectory for long enough times, break it up into shorter pieces, sum over the short pieces, and so obtain the microcanonical correlation function. Such a scheme is based on the ergodic therorem which assures that phase-space averages are identical with time averages. We have undertaken a thorough study of the spectra of chaotic bound and dissociative trajectories of the H_3^+ system on the DIM potential energy surface. Although such spectra do have a broad structure,[7,10] it proved impossible to resolve features with a resolution of a few inverse centimeters, which would correspond to the experimental coarse-grained spectrum. Chaos is simply too strong and correlations die out much faster than the correlation time needed to produce a peak of width 5 cm^{-1} (7 ps), which is the width of the experimental coarse-grained spectrum.

The approach outlined above assumes implicitly that all of phase space is chaotic. In fact, our studies of the periodic orbits of nonrotating H_3^+ showed that there exists one type of periodic orbit that is stable. Trajectories initiated in its close vicinity stay there forever and *do not visit all of phase space*. Thus, for $J = 0$ we already know that phase space must be decomposed at least into two different parts that do not mix, so the $J = 0$ dipole spectrum is a sum of the spectrum from the chaotic sea, and one from the phase-space portion of the regular manifold localized around the periodic orbit. We termed this orbit "horseshoe" because of its configuration-space path (cf. Figure 6). The motion of this orbit is a vibration in C_{2v} geometry which can be described as a bend of collinear H_3^+ with the unusual property that the bond lengths between the outer H's and the middle H are strongly shortened while bending. Since motion in the vicinity of this orbit is quasiperiodic, the dipole spectrum of such trajectories consists of a series of sharp peaks, which must be superimposed on the broad background coming from the chaotic part of phase space, before comparison with experiment.

It was found (using a novel adiabating switching method[10]) that the "horseshoe" vibration remains stable even if the two outer atoms are rotated about the C_2 axis, i.e., the line of motion of the central atom. The case $J = 10$ is shown in Figure 6. Thus the abovementioned division of phase space into two nonmixing regions holds at least for any $J < 20$. Since rotation and vibration of these "rotating horseshoes" are strongly coupled, this rotation modulates the vibrational spectrum with its frequency, thus producing "sidebands" in the spectrum. When this rotational frequency is computed (and semiclassically quantized) on the accurate energy surface of ref 37, it turns out[9,10] to be near 50 cm^{-1}. We conclude that the ~50-cm^{-1} splitting in the coarse-grained spectrum is just a reflection of the rotational constant of the "rotating horseshoe" orbit.

This interpretation of the coarse-grained spectrum is quite different from early attempts,[17] which noted that there exists a series of rotational $j = 3$–5 transitions of the H_2 molecule that give the same spacing and assumed a loose $H_2 \cdot H^+$ complex as the structure of the observed H_3^+. Our interpretation implies that the spectrum results from motion of a tightly bound H_3^+ molecule that is rotating, and has very little to do with the motion of free diatomic H_2.

It should be stressed that the stable phase space surrounding the rotating horseshoe is very small. This means that the magnitude of the peaks coming as a result of the stable manifold is very small when compared to the chaotic background. Similarly, the experimental coarse-grained spectrum consists at most of a few hundred lines out of the 27 000 lines measured.

In summary, a classical mechanical theory of coarse-grained spectra leads to a simple assignment of the experimental peaks. The theory is though by no means complete. One of the most difficult tasks is finding all stable manifolds. There is, to date, no fully consistent method of enumerating all periodic orbits in a system as complex as H_3^+. We found the stable manifold by studying periodic orbits in high-symmetry subspaces of the system such as the collinear and C_{2v} configurations. Such a methodology should also prove useful for other more complicated molecules such as acetylene.[33]

V. Discussion

The detailed photodissociation experiments on metastable H_3^+ provided a theoretical challenge that has been largely answered. At present, it is the theory that is returning the challenge to the experiment. As mentioned in the Introduction, the basic mechanism for formation of metastables is quite general. The decay is determined by tunneling through total J barriers. Intuitively one might expect that such tunneling phenomena would only be observed in light atoms such as hydrogen. However, the analysis of Klots[20] as well as recent experiments on Ar_3^+ clusters[24] indicates that tunneling can also be detected in heavy fragments. As already noted, tunneling of deuterium has been detected in H_3^+. Experiments on heavier metastables would be of great interest. The fragmentation of larger metastables and the dependence on total J could turn out to be of practical use in the control of unimolecular dissociation and in the separation of the fragments. Such studies could easily be augmented by theory since, as we have seen, mostly classical trajectory techniques or transition-state theory suffices. These are not strongly limited by the dimensionality of the system.

Specific predictions have also been made for the H_3^+ system. Foremost, the experiment should be redone with a careful measurement of the correlation of prod-

(37) Meyer, W.; Botschwina, P.; Burton, P. *J. Chem. Phys.* **1986**, *84*, 891 and private communication.

uct translational energy distribution with the identity of the fragment. For the HD_2^+ or H_2D^+ systems, such a correlation would serve to verify our predictions on the mechanism. Low E_T will lead to H^+, high E_T to D^+. A measurement of the crossover would provide important information with which to test the quantitative accuracy of the theoretical analysis.

The study on "rotating horseshoes" indicates that the coarse-grained spectrum is associated with low-J states. Since no more than 500 lines are responsible for the prominent peaks, a detailed study of the translational energy distribution associated with this specific set of lines would serve to verify the proposed classical model. Our studies have shown that classical trajectories may be used to interpret the experimental spectrum. However, the quantum correspondence is not yet fully understood. Taylor and co-workers[35] have suggested that coarse-grained features of high-energy spectra should be analyzed in terms of Feshbach resonances. The nature of the resonance Hamiltonian associated with the rotating horseshoe as well as questions such as whether this resonance Hamiltonian can support enough resonance states to be consistent with experimental observations remains open for future research.

In summary, we expect that the beautiful experiments of Carrington and Kennedy, augmented by our analysis, will open up a new avenue of research into the dynamics of metastable ions and molecules.

We are indebted to our collaborators Dr. J. M. Gomez Llorente and Dr. M. Berblinger for their insight and enthusiasm. We thank Prof. M. S. Child for his comments on this manuscript. This research has been generously supported by the U.S. Israel Binational Science Foundation, the Minerva Foundation, and the Deutsche Forschungsgemeinschaft.